KCFP Final Report 2018-2022

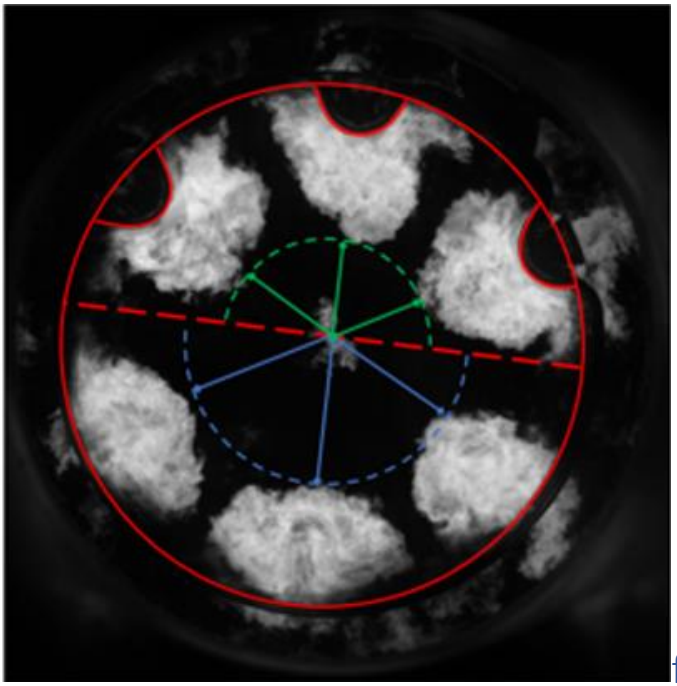

ff

Table of Contents

Introduction

The purpose of KCFP is to conduct high-quality academic research in close collaboration with automotive industry within the fields of combustion and thermodynamics for engines in order to contribute to an efficient, sustainable and competitive transportation system.

Advanced methods for analysis, measurements, simulations and synthesis as well as a high-class engine laboratory contribute to improve the understanding of fundamental phenomena which enables researchers within KCFP to identify new technological possibilities and solutions for combustion and thermodynamic systems in engines.

In KCFP, new concepts and understanding of fundamental processes are generated which manifests itself in both physics-based and phenomenological models. This is enabled by access to unique experimental and computational resources. The activities within KCFP are conducted in line with the long-term priority of a fossil-independent transportation fleet by 2030 as an intermediate step towards the vision of a fossil-free Sweden by 2050.

KCFP should support Swedish automotive industry and other stakeholders with relevant innovative research with a main horizon of 10–15 years. This does not exclude individual activities and projects with a shorter time perspective.
KCFP should be a stable and efficient long-term foundation for research, education and societal interaction. The center should recruit and educate future technical leaders and experts. The width of competences is ensured through collaboration between researchers within the center where four academic subjects are represented (combustion engines, fluid mechanics, combustion physics and automatic control) as well as collaboration with experts from industry and society at large.

The final report of KCFP consists of this annual report for the extended final year 2021-01-01 – 2022-06-30 together with the previous annual reports for 2018, 2019 and 2020.

Vision and mission

The KCFP vision is to generate knowledge and methods that contribute to making the combustion engine an environmentally sustainable alternative in future transportation systems. More specifically this means that net emissions from combustion engines with exhaust aftertreatment should be zero regarding:
Harmful emissions (nitric oxides, particles, carbon monoxide and hydrocarbons)
Greenhouse gases

In addition to the zero vision regarding emissions, the research is driven by a vision of combustion engines that are substantially more energy efficient than today’s engines and that are suitable for broad implementation in the transport system.

In KCFP the challenge of the zero vision regarding emissions from combustion engines is met with leading edge research on combustion and thermodynamics in engines. The research within KCFP is directed towards new technologies and methods that can contribute to substantial improvement in energy efficiency, zero emissions in real operation and 100% renewable fuels.

- KCFP should conduct multidisciplinary research with collaboration between academy and industry in order to create a positive vision that inspires innovative technological solutions
- for sustainable transportation. KCFP should also educate experts in the fields of combustion and thermodynamics for engines.

- KCFP should conduct research to facilitate a transition to more knowledge- and research-based methods in order to reduce development times for more efficient, cleaner and,
- if applicable, hybrid drive trains powered to a substantial extent by renewable fuels.

Goals

The main goal of the program is to generate research results and knowledge that, over a 10–20 years horizon, enables:
development of zero-emission combustion engines (zero vision)development of combustion engines for fossil-free fuels with at least 53% brake thermal efficiency over a substantial part of the operating range
development of combustion engines that, together with a hybrid drive train, consume 20% less fuel relative to today's conventional drive trains
development of fossil-independent combustion engines for transportation over land and sea and production of heat and power

The goal of KCFP is to be a leader both in Sweden and internationally regarding thermodynamics and combustion in engines.

Important events during 2021 and 2022

Two "KCFP Days" events were conducted during 2021, one in May and one in November. Both featured one full day of research seminars as well as open discussions about the activities in the center. Due to the pandemic, the May event was conducted entirely online whereas the November event had on-site participation. A keynote presentation on LCA analysis was delivered by Prof. Öivind Andersson during the May event. For the November event, Dr. Edouard Berrocal delivered a keynote presentation on recent developments in spray diagnostics.

Since 2021 is the last year of KCFP the activity level is quite reduced compared to a few years ago. It was also decided to formally extend the KCFP program period to June 31, 2022 which means that this report is for 2021 and the first half of 2022. Our excellent chairman for many years of KCFP, Sören Udd, decided to retire after 2021 as originally agreed and was replaced for the last half year by Dr. Johan Engström from Volvo.

One new project on ignition and spark plug wear in natural gas / biogas engines was initiated during 2021 which will also generate some additional in-kind contributions from industry. It has been recognized that there is an important trade-off between ignition quality and spark-plug wear, but recent development of controllable AC capacitive discharge ignition systems may somewhat alleviate this trade-off and provide both adequate ignition quality and acceptable wear.

During 2021 and 2022 the following PhD students were awarded their doctoral degrees:

- Carlos Jorques Moreno based on the thesis “Design and Optimization of In-Cycle Closed-Loop Combustion Control with Multiple Injections”
- Shijie Xu based on the thesis “Large eddy simulation of dual-fuel combustion under ICE conditions”
- Alexios Matamis based on the thesis “Optical and laser diagnostics : The versatility of Imaging”
- Manu Mannazhi based on the thesis ” Laser-based diagnostics for investigating soot formation in combustion processes”
- Xiufei Li based on the thesis “Learning control for flex-fuel CI engine and fuel cell”
- Menno Merts based on the thesis ”Advancing the understanding of pilot ignition in dual fuel engines : Experimental and conceptual studies”
- Nika Alemahdi based on the thesis ”ϕ-sensitivity - A step forward in future fuels evaluation”

Consequences of COVID-19

COVID-19 arrived as an unpleasant surprise towards the end of 2019 but developed into a full-fledged pandemic in the beginning of 2020 with severe consequences for people’s health, lives and the world economy. Not surprisingly, the pandemic has had severe implications also for KCFP with cancelled and interrupted research stays, both incoming and outgoing. Work in the engine laboratory was during most of 2020 restricted to a bare minimum and the normal hallway and coffee break discussions that are so important for creativity were reduced to scheduled discussions in Teams and Zoom meetings. The KCFP Days were also limited to online events instead of the normal on-site events. The contacts with our research partners were severely hampered by different levels and durations of shutdowns. After summer in 2021 life began to normalize thanks to large-scale vaccinations and we were able to host an on-site KCFP Day in November 2021. All restrictions have gradually been lifted as well.

Organization

Board

Sören Udd, Chairman, Johan Engström, Malin Ehleskog, AB Volvo, Carolin Wang-Hansen, Håkan Persson, Volvo Car Corporation AB, Per Stålhammar, Hualu Karlsson, Scania CV AB, Heiner Linke, Maja Novakovic, Lund University, Sofia Andersson, Anders Johansson, Swedish Energy Agency

Members

The following organizations have been members of KCFP during 2021 and 2022: Lund University, The Swedish Energy Agency, Scania CV AB, Volvo Car Corporation AB, AB Volvo, Cummins Inc., Loge, Wärtsilä Finland Oy, SEM AB, Convergent Science Inc., Metatron

KCFP research staff

The following PhD students and postdocs have had a substantial part of their research activity within KCFP during 2021 and 2022. Saeed Derafschzan, Alexios Matamis, Xiufei Li, Menno Merts, Ola Björnsson, Mike Treacy.

Research

There are obviously many logical ways to split the research activities within KCFP. Based on the frequencies of certain keywords we found it logical to split the content into “Compression Ignition” and “Spark Ignition. Needless to say, nearly all contributions use alternative and/or renewable fuels which makes such a category useless to organize the content.

Compression Ignition

Three flavors of compression ignition are reported: dual fuel combustion, PPC combustion and spray driven combustion. These three combustion modes are respectively studied with three different methods: single cylinder thermodynamic engine studies, detailed CFD models and optical methods.

Experimental optimization of a medium speed Dual Fuel engine towards RCCI operation – Metal campaign.

Researcher: Menno Merts

Objectives

To increase the understanding of pilot ignition in a medium speed dual fuel engine, optical research is performed on a Wartsila W20DF marine engine. To support this optical work, a metal campaign is performed. The objective is to create insight in the behavior of emissions, in the operating range from RCCI to Conventional Dual Fuel. The found optima can be used in a future optical campaign.

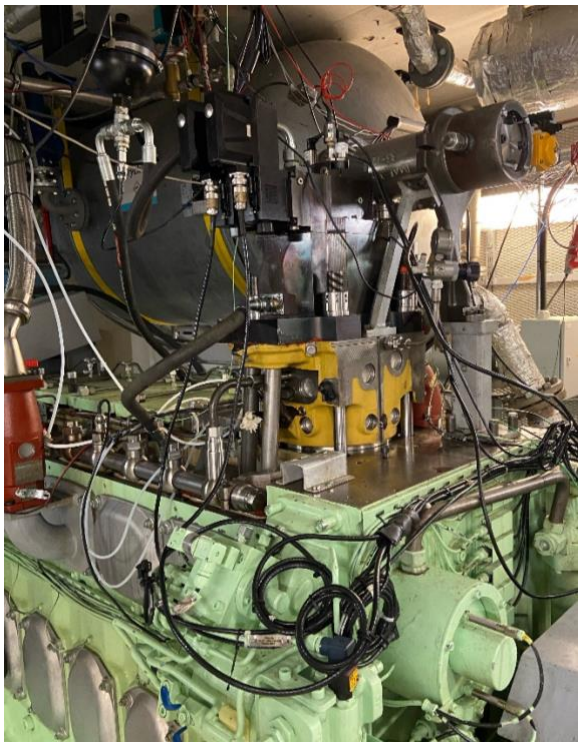

Figure 1: Wärtsilä W20DF test engine at Lund University.

Introduction

The ongoing energy transitions results in a growing interest in renewable fuels. What most renewable fuels have in common is that they are high octane fuels, while the market of marine and industrial engines mainly consists of CI engines. They require a low octane fuel. The dual fuel concept allows the application of renewable fuels like biomethane or methanol in a diesel engine. Parameters of the pilot injection have a strong impact on the emissions and performance of the engine. By advancing the timing of this injection, the engine can run in RCCI mode instead of conventional dual fuel. A first optical analysis of the effect on combustion behavior was already performed on the engine in Bowditch setup. Running in skipfire mode prevented the measurement of emissions. For that reason, the engine was built back to metal configuration, and a new experimental campaign was performed.

Method

The Wartsila W20DF 200mm bore 6-cylinder engine in TC12 at Lund University was running as metal engine, operating on 1 cylinder. The turbocharger was mimicked by buffered pressurized intake air, and an adjustable exhaust gas backpressure valve. The engine was running on direct injected Swedish MK1 diesel fuel and port injected natural gas from the South Swedish gas net, where above 95% of energy was supplied by natural gas. Engine-out emissions were measured with a Horiba MEXA 9400 setup, measuring CO and CO_2, NO_x, HC, and O_2. The measurements were performed constant fuel inputs on three reference loads, 10, 14 and 18 bar IMEP. For each reference load a sweep of the Start of Injection of the pilot fuel was made. Tests were performed at a global lambda of 2.

Results

Initial the advancing of the start of injection away from TDC results in an advancing of the combustion process. This early combustion phasing, where a significant amount of energy is released in the small volume around TDC, results in an increase of NOx emissions. At the same time this phasing and its high peak temperature lowers the emission of uHC. When injecting earlier than ~30 cad bTDC, more time is created for dilution of the pilot fuel, resulting in RCCI combustion. The strong premixing increases ignition delay and results in a later phasing of the combustion process. The following more gradual heat release profile reduces NOx emissions, where raw engine out values below 2g/kWh can be achieved. It is at this timing where also the highest indicated efficiency can be found, caused by a combination of low heat loss, complete combustion and proper combustion phasing. Further advancing of the pilot gives the disadvantage of too strong dilution, resulting in an increase of uncombusted methane emissions. Only at low load a sweep over the full SOI range could be achieved. Both in the medium and the high load case the injection timing in the experiments was limited because of combustion knock.

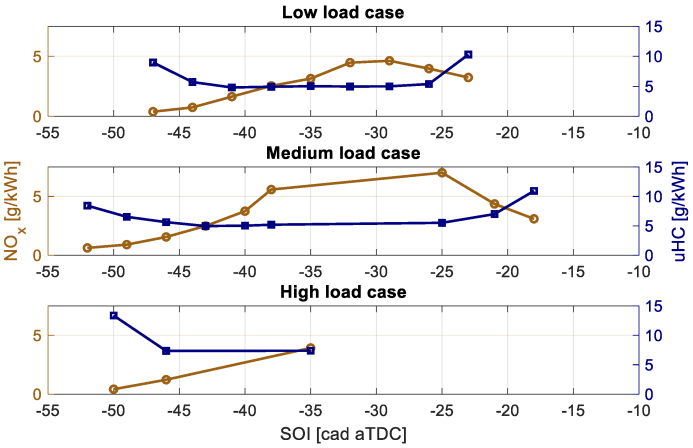

Figure 2: Emission dependence on start of injection timing at different loads.

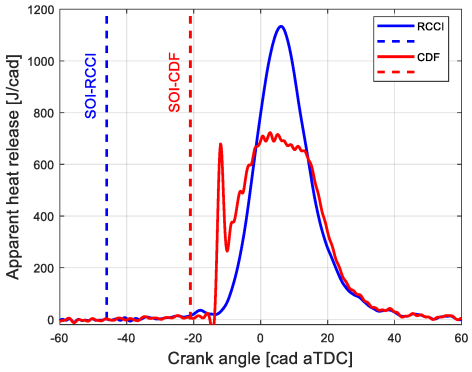

Figure 3: Combustion characteristics with RCCI combustion and CDF respectively.

Conclusions

An optimum combination of low NO_x emissions and efficiency can be achieved with a very early pilot injection. In the resulting RCCI combustion mode a strong premixing of the pilot injection prevents an initial peak in heat release.at late RCCI timing. Too early injection, where even more dilution of the pilot takes place, the emission of uncombusted hydrocarbons strongly increases and efficiency drops off.

RCCI operation, and its gradual heat release profile strongly reduces the knock sensitivity of the engine.

A strong correlation between the emission of uncombusted hydrocarbons and cycle to cycle variation was seen. This could give the possibility to use the COV of IMEP as an observer, in optical experiments where emissions could not be measured.

The desired operating points for a future optical campaign were defined for low, medium and high load.

Publications

M. Merts, B. Veenhuizen, M. Lundgren, and S. Verhelst, “Experimental optimization of a medium speed Dual Fuel engine towards RCCI operation.,” presented at the Thiesel 2022, Valencia, Spain, Sep. 2022.

M. Merts, “Advancing the understanding of pilot ignition in dual fuel engines: Experimental and conceptual studies,” PhD Thesis, Division of Combustion Engines, Lund Institute of Technology, 2022.

Wave Piston Project, Optical Diagnostics

Researcher: Saeed Derafshzan

Research goals

The role of a novel piston shape designed by Volvo, has been studied in Volvo D13 optical engine. Multiple diagnostic techniques were utilized to capture flow field inside the piston bowl, air-fuel mixing, ignition, and combustion. Particle image velocimetry (PIV) was used to get the flow field from the injection and mixing and during different stages of the combustion. Combustion natural luminosity (NL) was recorded simultaneously, which focused on the effects of wave-piston design on combustion behavior.

Introduction

With ever growing demand for reducing the negative impacts of combustion processes in different industries, huge efforts have been put in making internal combustion engines more efficient. This efficiency not only leads to a better energy conversion, but also reduces unwanted emissions which is vital for the future of internal combustion engines. Design and optimization of piston bowl shape is one of many ways to achieve these goals. A novel piston design with protrusions inside, called Volvo wave-piston, is implemented which proved promising in enhancing mixing, and decreasing soot. In this project, an optical wave-piston with similar design is utilized in a Volvo D13 heavy duty optical engine and the effects of wave design have been studied extensively.

Methods

High-speed imaging of NL and PIV techniques were used simultaneously to investigate combustion processes and the flow inside the combustion chamber, respectively. Laser beam from a dual-cavity Nd:YLF laser creates light sheet, and the scattered light from the TiO_2 particles that are seeded into the intake manifold, is recorded with a high-speed CMOS camera. A second high-speed CMOS camera captured NL simultaneously. Furthermore, cylinder pressure, rate of heat release (RoHR) and other engine-running parameters are measured and derived. The fuel used here is n-Heptane and exhaust gas recirculation (EGR) was utilized in some of the cases to lower soot and make the PIV experiment in reacting conditions possible.

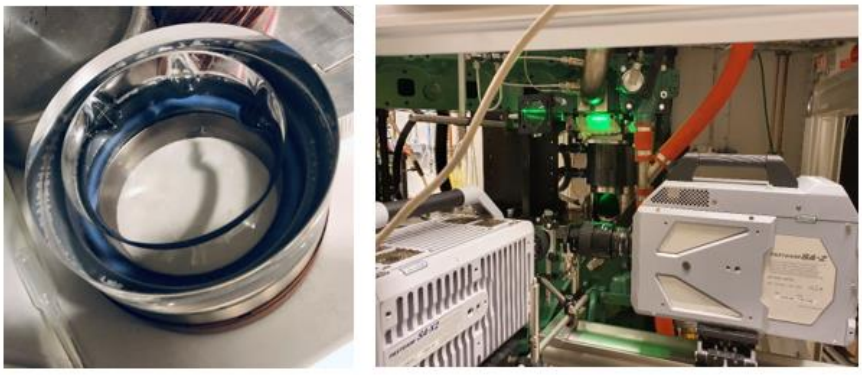

Figure 4: Optical wave-piston (left) and the experimental setup (right)

As visible in Figure 4, the slight difference between glass wave piston replica compared to the metal version is that wave protrusions only exist on one side of the piston for technical

reasons. This difference creates a great situation in which the effect of wave-side and flat side of the piston is visible within the same cycle.

Results

In the following figures, the differences between wave side (top of the images), and flat side (bottom) are discussed. Averaged NL images during ignition and CA50 along with cylinder pressure and RoHR can be seen in Figure 5.

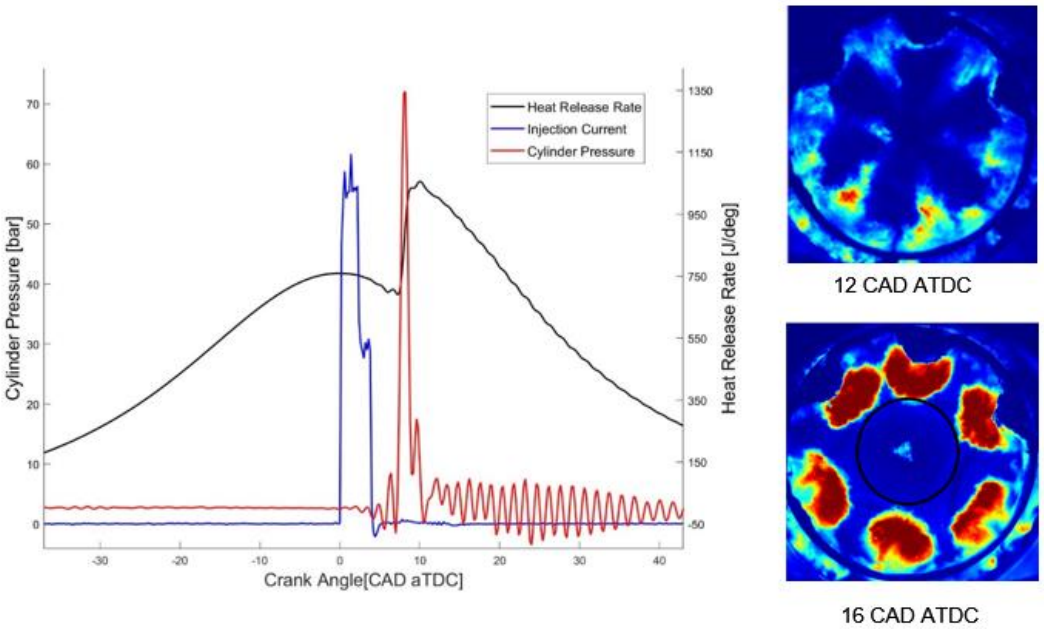

Figure 5: Cylinder pressure and RoHR (left) and NL images (Right)

A clear difference caused by the waves is in how closer the flames on the wave side get to the center of the piston bowl. Better air utilization due to waves, along with late cycle soot oxidation, are amongst the explanations for lower soot emission in this piston design. In Figure 6 this effect is depicted. First, larger flame stretch on the wave side is visible (top, left), and the stretch is graphed at different CADs (top, right). And the spray, ignition and combustion phasing and the differences are captured (bottom).

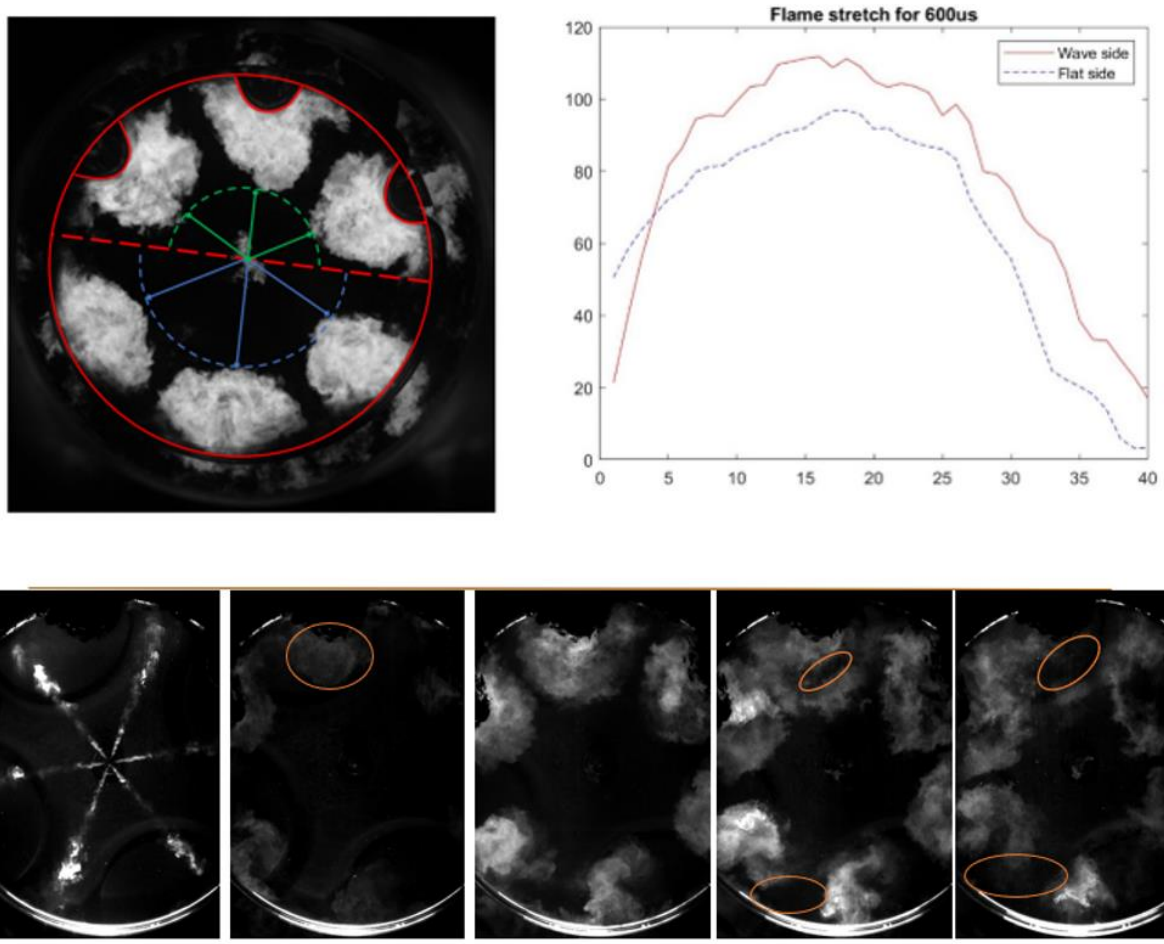

Figure 6: NL image of wave and flat side (top, left), air utilization defined as flame stretch (top, right) and different stages of the cycle (bottom)

Conclusion

To better understand the mechanisms behind the improvements of wave piston design, i.e., lower soot emissions and better mixing, different optical diagnostic techniques have been used. Some of the findings are listed below.

- Wave protrusions create a clearly different pattern in mixing, via different jet-wall and jet-jet interactions of the fuel.
- These differences have been tracked from the injection throughout the cycle via different techniques, including NL high-speed imaging and PIV.
- These effects further on leads to differences in combustion phasing, in which the wave-side had better air-utilization followed by more soot oxidation later in the cycle.

CFD modelling of PPC engine combustion

Researchers: Mark Treacy, Leilei Xu
Supervisor: Xue-Song Bai

Objectives

Gasoline and methanol are prominent fuels for low temperature combustion (LTC) strategies because of their high research octane number (RON) allowing early injection timings without risk of engine knocking. There have been a number of metal engine experiments and optical engine experiments on gasoline and methanol PPC engines, which showed significant dependence of engine performance (combustion efficiency and indicated thermal efficiency) and emissions (CO, NOx and unburned hydrocarbons, UHC). However, there is significant knowledge gap on the combustion process in PPC engines, e.g., on mechanisms of emission formation and modes of reaction front propagation. The objective of this CFD project was to perform 3D and time dependent numerical simulations of the fuel injection, evaporation, mixing and combustion process in PPC engines, and using the numerical data to gain deeper insight to the performance and emissions of PPC engines operating with different fuels (gasoline or its surrogate and methanol).

Introduction

LTC strategies aim at reducing pollutant (NOx and soot) emissions by reducing in-cylinder temperatures and enhancing the in-cylinder fuel/air mixing (to reduce the fuel-rich mixtures). LTC can be achieved by injecting the fuel into the combustion chamber earlier in the stroke compared to the conventional diesel cycle (CDC). Very early injection provides a long mixing time producing a fuel lean homogeneous fuel/air mixture when ignition occurs, which is referred to as homogeneous charge compression ignition (HCCI). Partially premixed combustion (PPC) is another LTC strategy achieved by early injection. However, the injection occurs between the HCCI and CDC ranges providing some level of additional mixing without achieving fully fuel/air homogeneity. Typically, low RON fuels (such as diesel) are used in CDC cycles due to their ease of ignition; however, high RON fuels are more suitable for LTC as they have a greater resistance to auto-ignition, reducing the chance of pre-ignition, expanding the start of injection (SOI) window, and allowing for higher compression ratios. Gasoline is a prevalent high-octane number fuel. However, with significant interest in renewable fuels, alcohol fuels such as methanol are recommended as an alternative fuel for PPC engines. Methanol is particularly suitable for PPC engines as it has a slightly higher RON than gasoline, promotes charge cooling by absorbing a large amount of heat during the evaporation phase and also can achieve lean mixtures faster than gasoline due to its low stoichiometric air/fuel ratio. However, the lower heating value (LHV) of methanol requires almost twice the fuel mass of gasoline to be injected into the combustion chamber in order for the same amount of energy to be injected into the cylinder.

Within KCFP research program, a series engine experiments have been carried out to investigate the PPC engine performance when operating with gasoline surrogate [1-3]. When operating the PPC engine with different injection timing, the combustion timing (CA50 – crank angle at which 50% of heat is released) is often kept constant (i.e., slightly after top-dead-center, TDC). Figure 7 shows that the intake temperature needs to be varied in order to maintain a constant CA50. Figure 8 shows that the engine-out emissions are strongly dependent of the injection timing, with UHC and CO showing non-monotonic variation at different injection timing, whereas NOx shows an increasing trend with delayed injection. To understand the engine performance and emission trend, and to bridge the knowledge gap in

the fundamental combustion process, e.g., modes of reaction front propagation, detailed numerical simulations are carried out. The numerical simulations are presented in three publications [1-3], where presentation of the detailed numerical methods and numerical results can be found. In the following highlights of the results are presented, which are divided into two subsections: (a) analysis of engine performance and emission in PPC engines operating with iso-octane (gasoline surrogate) and methanol, (b) analysis of the modes of reaction front propagation in PPC engine operating with PRF70 (gasoline surrogate) fuel.

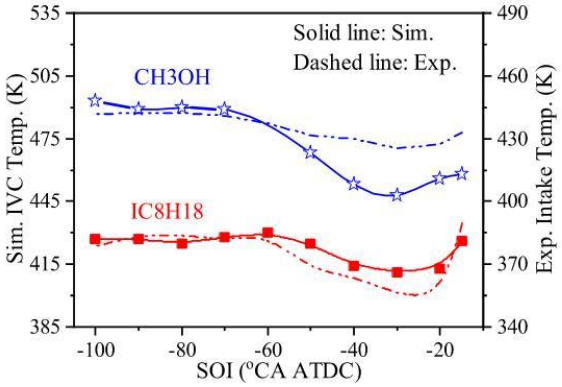

Figure 7: Comparison of the required IVC temperature from CFD simulations and ensemble-averaged intake temperature from the experiment on Scania D13 engine at different SOI with CA50 around 3◦ CA and operating with different fuels.

D13 engine at different SOI with CA50 around 3◦ CA and operating with different fuels.

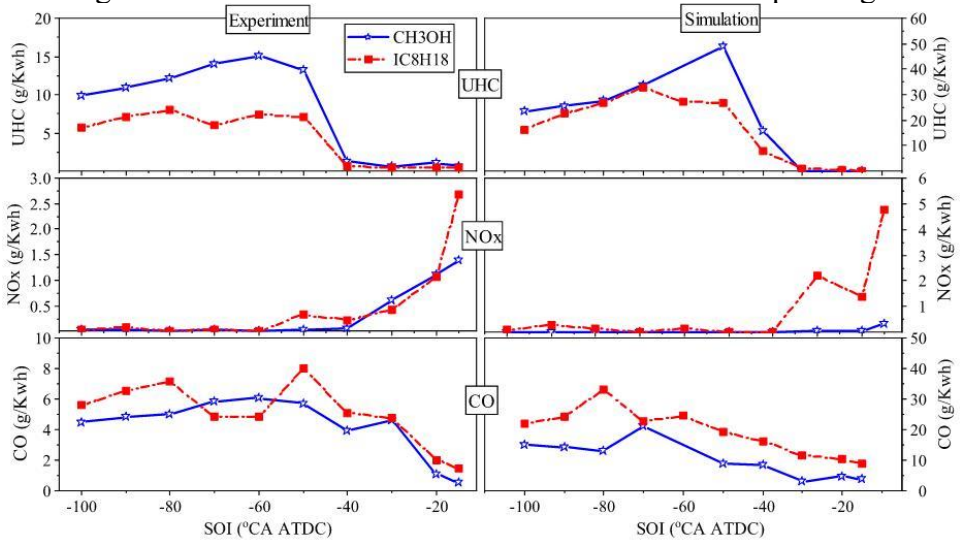

Figure 8: UHC, CO and NOx emissions from Scania D13 engine under different injection timings. The results are from engine experiment and CFD simulations.

Methods

Analysis of engine performance and emission in PPC engines operating with different fuels

CFD simulations were carried out using OpenFOAM V7 on the Scania D13 heavy duty direct injection engine. The engine has a bore/stroke length of 130/160 mm and a connecting rod length of 255 mm achieving a compression ratio of 17:1. The fuel was injected at 800 bar through 12-hole injector with a hole diameter of 230 µm and an umbrella angle of 120°. The intake temperature was adjusted to maintain combustion phasing of CA50 at 3° CA. Due to the higher required fuel mass of methanol, a longer injection duration then iso-octane was required. The engine was operated without EGR and the LTC ranges were realised by

carrying out an SOI sweep from -100°CA aTDC to -10°CA aTDC in 10°CA increments, covering three regimes of combustion: HCCI, PPC and transition regime from HCCI to PPC. A modified generalized re-normalised group (gRNG) k-ε turbulence model was used with the fuel spray modelled using the Langrangian-Eulerian approach. A 30° sector of the full cylinder was used, which represents a single spray plume. The case was carried out between intake valve closing (IVC, -141°CA aTDC) and exhaust valve open (EVO, 137°CA aTDC). An add/remove mesh algorithm was implemented to add and remove cells based on their height, reducing cell count, and improving mesh quality throughout the simulation.

Results

The intake temperature was predicted and it was found that both fuels a 'spoon shape' trend (Fig. 1), where the handle of the spoon is located in HCCI regime and the curve of the spoon is formed in the transitional regime and PCC regime. Overall, methanol requires a higher intake temperature than iso-octane due to the evaporative cooling effect of methanol. A higher intake temperature is required in the HCCI regime as a higher temperature is required to ignite the homogeneous fuel-lean mixture. The transitional regime forms both fuel-lean and fuel-rich pockets. The fuel-rich pockets require less temperature to ignite, explaining the lower intake temperature in this regime. The PPC regime requires a higher intake temperature in order to heat the charge more quickly as a result of the lower IDT in the other regimes. The emissions for both fuels can be seen in Fig. 2, where the experimental data is on the left and the simulation on the right, with red representing iso-octane and blue methanol. The simulations can be seen to be able to capture the trend for the emissions of unburned hydrocarbons (UHC), nitrous oxide (NOx) and carbon monoxide (CO). The spray during the HCCI phase impinges on the cylinder wall and the fuel becomes trapped in the crevice region away from the main combustion region and cannot be ignited and is the reason for the high UHC emissions in the HCCI phase. The sudden drop in UHC emissions is due to the spray being targeted in the cylinder bowl where almost the entirety of the fuel is burned. The main formation of NOx emissions is in the mixture where in-cylinder temperatures are over 1800 K. The long IDT for the HCCI and transitional phase allow for greater mixing which leads to fuel-lean mixtures that is burned at a lower temperature where NOx does not form. As the SOI is retarded, fuel-regions become more frequent due to the reduced level of mixing. Fuel-rich burn at a higher temperature and hence, the formation of NOx is higher for the cases where IDT is lowest, in the PPC regime. The formation of CO is dependent on the equivalence ratio of the mixture. Overly fuel-rich or fuel-lean zones can prevent oxidation and result in high CO output. The high CO emissions observed in the HCCI regime are a result of some overly fuel-lean regions and/or low-temperature regions which cannot be fully ignited. As the SOI is retarded, the charge becomes less fuel-lean and the CO emissions drop with retarded SOI. During the PPC regime, where CO emissions are lowest, the mixture is around stoichiometry and the combustion temperature is highest such that CO is oxidised into CO2 and the output of CO is lowest of all cases.

Further details of the results are referred to published papers [1-2].

Analysis of the modes of reaction front propagation in PPC engine

CFD simulations were conducted in an optical PPC engine fuelled with the PRF70 fuel (70% iso-octane, 30% n-heptane by volume). The main objective of this study was to gain a comprehensive understanding of the ignition process and flame structures in gasoline PPC engines. The numerical simulation was based on a five-dimension Flamelet-Generated Manifold (5D-FGM) tabulation approach and large eddy simulation (LES). The goals were to identify the different combustion modes, as well as the dominant chemical species and elementary reactions involved in the PPC engines, and to understand the impact of injection strategies on the engine performance and emissions.

Methods

The simulations were conducted using an in-house solver developed for compressible turbulent flow on the computational fluid dynamics (CFD) platform OpenFOAM-V7. The fuel spray process was modeled based on the well-established Lagrangian-Eulerian approach. The LES model consists of the spatially filtered continuity equation, transport equations for momentum, and FGM control variables. The sub-grid-scale (SGS) stress and transport fluxes were modeled using a one-equation eddy model based on the transport equation of SGS turbulent kinetic energy. The FGM combustion model adopted in this study was a tabulated chemistry modeling approach that was based on the flamelet concept. The local thermo-chemical properties were retrieved from representative laminar flames (called flamelets) according to selected FGM control variables. A counterflow diffusion flame configuration was applied to represent the turbulent non-premixed spray combustion. The flame equations were solved in physical space using CHEM1D. The control variables in the FGM model are the mixture fraction of the PRF70 fuel $\check{Z}$, the normalized progress variable $\check{C}$, the absolute enthalpy on the oxygen side $\widetilde{h_0}$, and the pressure $\check{p}$. Here, quantities with bar indicate spatially filtered, while with tilde they are density-weighted spatially filtered. This model is referred to as 4D-FGM, since it involves four control variables. To consider the different evaporation rates of the two fuels in the PRF fuel mixture, another control variable, $\widetilde{Z_2}$, which is the local mass fraction of n-heptane, was introduced. Since n-heptane evaporates faster than iso-octane, the volume ratio of the two fuels varies in space as will be discussed later. This spatially varying IC_8H_{18}/C_7H_{16} volume ratio has a significant impact on the low-temperature ignition process, and it has been neglected in the previous FGM literature. Finally, five control variables are stored in the 5D-FGM tables indexed by $\check{C}$, $\check{Z}$, $\widetilde{Z_2}$, $\widetilde{h_0}$ and $\check{p}$.

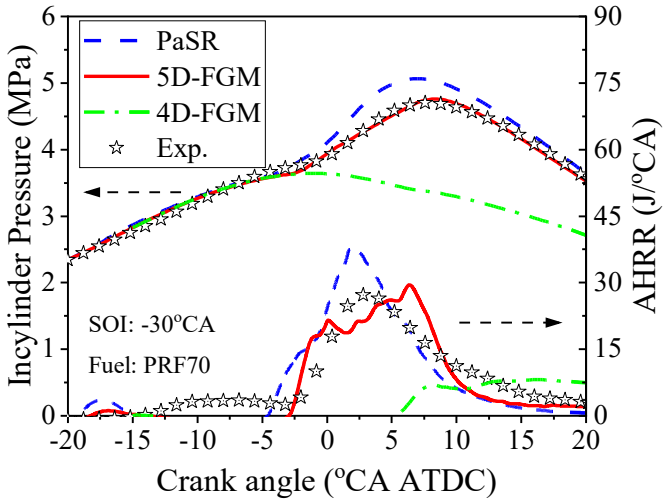

Figure 9: In-cylinder pressure and apparent heat release rate (AHRR) from the simulations and experiments.

Results

Validation of the simulation results was performed by comparing the in-cylinder pressure trace, and apparent heat release rate (AHRR) obtained from the experiment and the LES using the different combustion models, i.e., PaSR, 4D-FGM, and 5D-FGM, with the same initial and boundary conditions. As shown in Figure 9, after the fuel is injected into the cylinder, two heat-release stages can be found from the AHRR profile. The low-temperature ignition stage occurs in the crank angle range of -20 ~ -15 °CA. The high-temperature ignition stage starts slightly before the TDC, followed by a rapid heat release and pressure rise. With the same initial and boundary conditions, the 5D-FGM and PaSR models yielded similar results, while the 4D-FGM model predicted a very late ignition and poor combustion efficiency. Compared with the

experimental results, the results from the 5D-FGM model showed better agreement with the experiments in terms of the onset of high-temperature ignition, in-cylinder pressure and peak AHRR. The PaSR model predicted an earlier ignition and higher peak AHRR, resulting in a larger peak value of cylinder pressure. In the PaSR model, the transport equations for the entire species in the mixture are solved (135 species transport equations), which is time-consuming. The FGM model solves five transport equations for the control variables; thus, the computational time required in the FGM model is significantly lower than that in the PaSR model. The computational time of the present 5D-FGM model is about 10% of that required by the PaSR model.

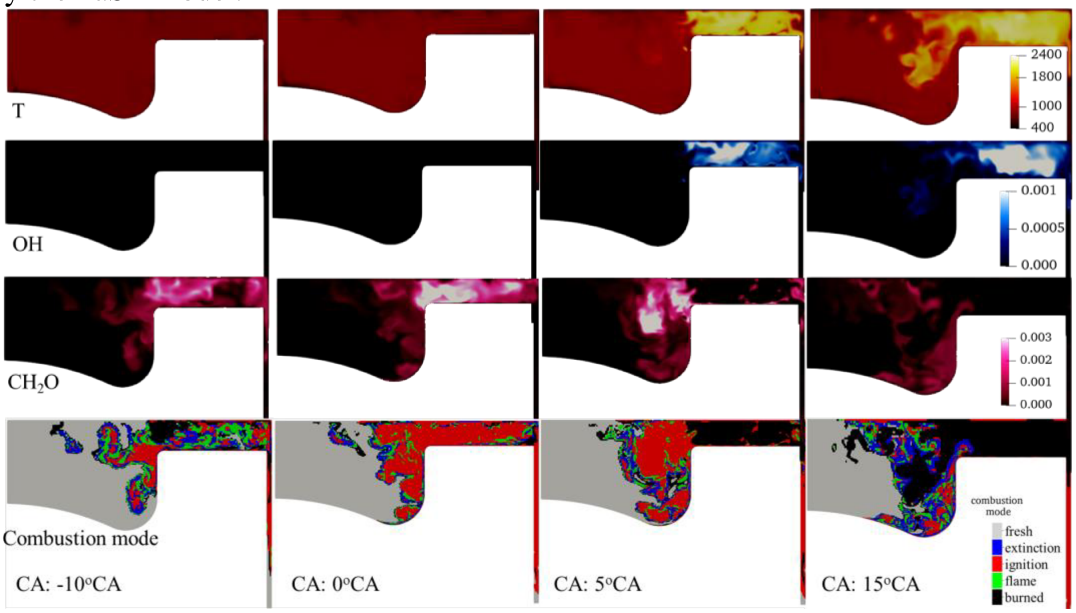

Figure 10: Spatial distribution of temperature, mass fractions of OH and CH2O, and local combustion modes identified by CEMA.

Figure 10 shows the instantaneous distributions of temperature and mass fractions of OH, CH_2O, and local combustion modes (identified using CEMA [4]) on the middle plane at different crank angles. At -10 °CA, a significant amount of CH_2O was already formed in the squish region. With the piston moving upward, the mixture temperature increases, and more CH_2O is produced and accumulated in the squish region. The temperature is still low and no OH radicals could be identified. In the CH_2O region, one can see multiple combustion modes, including chemically inert modes (burned region), ignition, extinction, and flame regions. The ignition is at its first stage (low-temperature ignition stage) and the flame is in a cool flame mode. The 'burned' region indicates where the first-stage ignition has ended and CH_2O has ended its production. Later at TDC in Fig.4, there are still no obvious OH radicals on the shown cross-section plane; the first stage ignition mode is the dominant mode in the combustion chamber, and the cool flame mode can also be identified in a thin layer surrounding the ignition mode region. At the CA50 (5 °CA), large amounts of OH radicals are already formed in the squish region where CH_2O is oxidized. Fuel in the squish region is almost completely oxidized and the mixture is therefore at the burned gas mode. In the piston bowl, a large region is in the first-stage ignition mode which results in the formation of CH_2O. The boundary of the ignition region shows a mix of cool flame propagation mode, extinction and burned gas modes. At 15 °CA, most fuel is burned and a large region remained unburned fresh mixture due to little fuel mixed with the air. In the boundary of the burned gas and unburned gas, combustion is at the flame mode. Since the unburned mixture in the high-temperature region mixes with the low-temperature air-rich region, and combustion is a mixing controlled,

thus at the diffusion flame mode. In the region near the wall of the piston bowl, a mix of cool flame propagation and first-stage ignition modes can be identified.
Further details about the method and results can be found in published paper [3].

References

[1] L. Xu, M. Treacy, Y. Zhang, A. Aziz, M. Tuner, X.S. Bai, Comparison of efficiency and emission characteristics in a direct-injection compression ignition engine fuelled with iso-octane and methanol under low temperature combustion conditions, Applied Energy 312, 118714, 2022.
[2] M. Treacy, L. Xu, H. Fatehi, X.S. Bai, Performance of a methanol fuelled direct-injection compression ignition heavy-duty engine under low temperature combustion conditions. 12th Mediterranean Combustion Symposium, Luxor, Egypt, January 2023.
[3] L. Xu, Z. Y. Zhang, Q. Tang, B. Johansson, M. Yao, and X.-S. Bai. LES/FGM investigation of ignition and flame structure in a gasoline partially premixed combustion engine. Proc. Combust. Inst. 39, 2022 (in press).
https://www.sciencedirect.com/science/article/pii/S1540748922002449
[4] T. Lu, C. S. Yoo, J. Chen, C. K. Law, Three-dimensional direct numerical simulation of a turbulent lifted hydrogen jet flame in heated coflow: a chemical explosive mode analysis, J. Fluid Mech. 652 (2010) 45‑64.

Low load ignitability of Methanol in a Heavy-Duty Compression Ignition Engine

Researcher: Magnus Svensson

Objective

The objective was to investigate the impact of a high compression ratio on low load ignitability of methanol in a CI-engine.

Introduction

With the majority of the maritime and transportation sectors using compression ignition engines fuelled with fossil diesel fuel (or heavy fuel oil), these sectors are responsible for significant amounts of greenhouse gases and pollutant emissions. One potential fuel that could make both sectors more environmentally neutral is methanol. It can be produced in renewable ways, and has properties making it possible to decrease greenhouse gases and pollutant emissions. It is also available in most ports today.

A challenge, when using methanol as a fuel in a compression ignition engine, is ignitability at low loads. The reasons for this are the low lower heating value (resulting in a longer injection) and high heat of vaporization together with a high octane number (hence very low cetane number).

The European Horizon 2020 project FASTWATER is looking to develop and demonstrate how methanol can be used in medium and high speed engines, with retrofit solutions and next generation systems. The research reported here is part of the FASTWATER work.

Method

This study sought to investigate ways of improving the ignitability of methanol at low loads, by testing the impact of a very high compression ratio. It started with comparing a simple methanol combustion strategy of pilot injection and intake heating to a simple diesel combustion strategy without pilot injection and with no intake heating, using a low compression ratio. Continuing on this, it investigated how a high compression ratio changed the low load ignitability of methanol and compared it to the lower compression ratio.

The investigation was performed on a Scania D13 heavy duty engine that had been converted to a single cylinder set-up of 2.12 liter swept volume, using two different piston set-ups: one with a geometrical compression of 17.3:1, for the low compression ratio, and one of 40:1, for the high compression ratio.

Results/conclusion

The experiments in this paper showed that methanol can be combusted in a CI heavy duty engine using retrofitting solutions of intake heating and pilot injection. This yielded good combustion and much lower NOx emissions than diesel, with only small differences in CO and UHC emissions which were close to or below legislation values. The experiment also confirmed that increased compression ratio can take away the dependency on intake heating and still yield good combustion with good efficiency at low loads, without compromising the emissions.

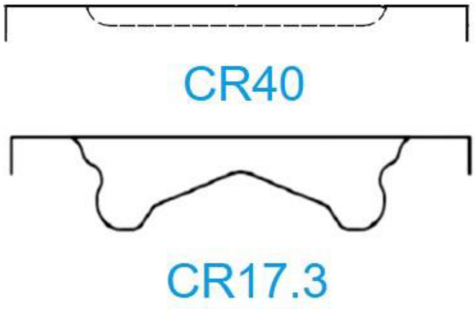

Figure 11: A schematic of the different piston bowls used.

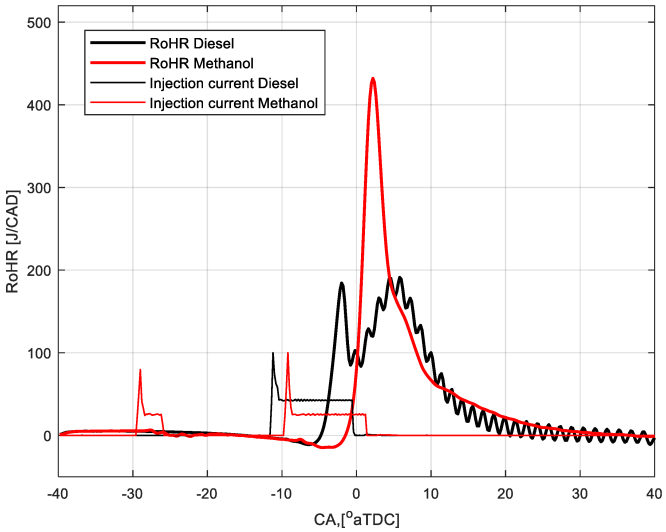

Figure 12: The RoHR, injection timing and length compared versus CA, at the CA50 timing of 5 for both diesel and methanol, for the low compression ratio and 6 bar IMEPg load case.

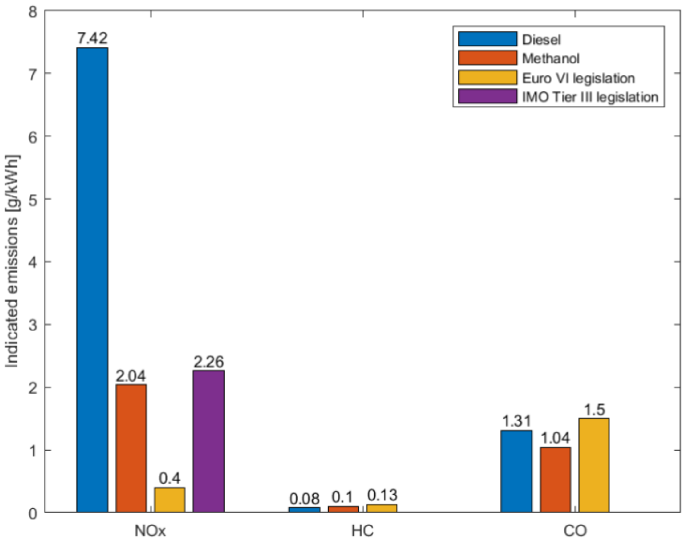

Figure 13: Indicated NOx, HC and CO for both diesel and methanol with the Euro VI heavy-duty and IMO Tier III engine emission legislation value, for the low compression and 6 bar IMEPg case.

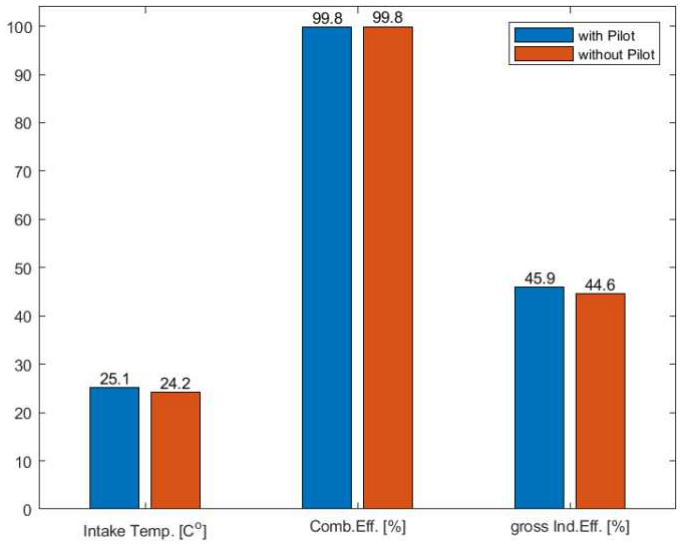

Figure 14: Intake Temperature, Combustion efficiencies and gross Indicated efficiencies, for methanol with high compression ratio and a load of 3 bar IMEPg, for with and without pilot injection.

Publication

Svensson, M., Tuner, M., and Verhelst, S., "Low Load Ignitability of Methanol in a Heavy-Duty Compression Ignition Engine," SAE Technical Paper 2022-01-1093, 2022, doi:10.4271/2022-01-1093.

Spark Ignition

Spark-ignited natural gas / biogas combustion is studied with focus on the ignition system. Ways to improve ignitability while preventing excessive spark-plug wear using flexible ignition systems are studied as well as how to extract valuable combustion information from the ignition system (ion current measurement).

Ignitability Study of Spark-Ignited Medium Speed Gas Engine

Researcher: Anupam Saha
Supervisor: Per Tunestål

Objective

A measurement campaign has been performed on the Wärtsilä W31SG medium bore gas engine. The objective of this research is to investigate and design an optimal spark for the engine at different operating points while achieving a robust ignition and a stable engine operation, even at highly lean/diluted conditions.

Introduction

Due to excellent knock-resisting properties of methane, the spark ignition (SI) combustion process is a good match for biogas fueled engines. Substantial effort is dedicated to make such engines a viable alternative and complement to electrification. One of the challenges in improving the thermal efficiency of an SI engine is the combustion stability at lean or diluted conditions. Concepts like multiple spark discharge and high ignition energy discharge improve ignitability, but may cause issues like enhanced spark plug erosion, fouling, and heat losses through the electrodes, which may adversely affect the performance and sparkplug lifetime. Therefore, an investigation has been performed by comparing a conventional DC ignition system with a novel AC ignition system, where the spark characteristics can be controlled by additional degrees of freedom. More specifically, this experiment campaign has been dedicated to study how the AC ignition system and its additional degrees of freedom affect ignitability and combustion stability. The specifications of the test engine setup are listed in Table 1.

Table 1: Specifications of the engine test bench.

Engine Type	**W31SG**
Cycle	4-stroke
Swept Volume	32.4 L
Injection Type	Port-Injected
Bore	310 mm
Stroke	430 mm
Length of Connecting Rod	1095.2 mm
Compression Ratio	11.7
A/F Ratio (Main Chamber)	Lean (Lambda ~ 2.0)
A/F Ratio (Pre-Chamber)	Lambda ~ 1.4
Nominal Power	600 Kilowatts @ 750 RPM
Distance (Coil Flange – Sparkplug)	860 mm (DC Inductive)
	970 mm (AC Capacitive)

Methodology

The sparkplugs used in this study is a standard J-gap design using iridium on both electrodes. In the first place, the DC Inductive ignition system was used in the experiment while the sparkplug of smallest available gap (0.22 mm) was mounted on the engine. At each EOP, the available spark control parameter(s) were successively decreased from high

to low energy level, until the engine performance (COV_{IMEP} as a measure) was below an acceptable level. The spark control parameters corresponding to the lowest spark energy for which $COV_{IMEP} \leq 2\%$ was recorded together with the corresponding engine performance parameters. Once the lowest spark energy profile was found for 0.22 mm sparkplug gap, the next available sparkplugs with higher electrode gaps were mounted and the experiments were then repeated at every EOP. Once, the tests were done using DC Inductive, the AC Capacitive ignition system was mounted on the engine and the experiments were repeated in a similar way, as discussed above.

Results

DC Inductive Discharge Ignition System

Figure 15 shows the coefficient of variation of IMEP – COV_{IMEP} (a) and peak pressure – COV_{PP} (b) of 300 combustion cycles versus dwell time sweep at 600 kilowatts brake power (100% engine load). It was found that once the combustion was stable enough, a further increase in dwell time (spark energy profile) did not improve both the COV_{IMEP} and COV_{PP} at different sparkplug gaps – tested. It was also noticed that the minimum required dwell time to achieve a robust combustion increased consistently with an increase in sparkplug gap, probably due increase in the required voltage to create a break-through between the electrodes' gaps.

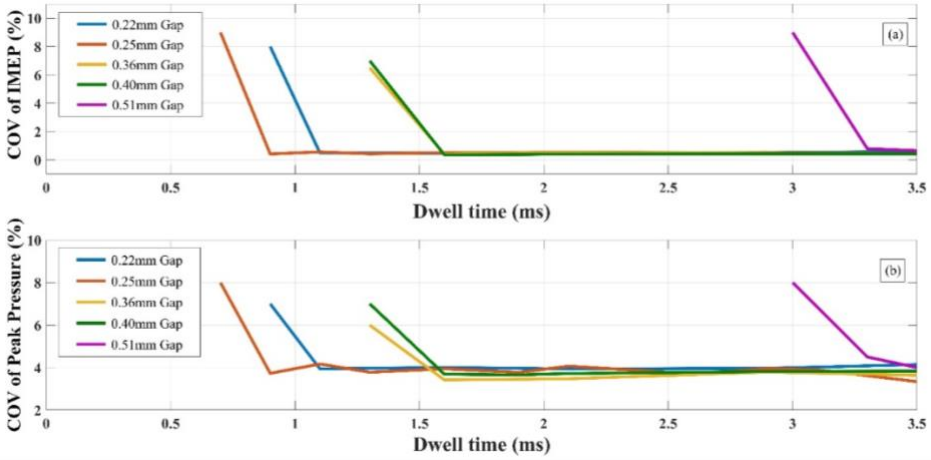

Figure 15: Top: DC Inductive – Dwell time sweep vs COV_{IMEP} @ 600 Kilowatts [100% Engine Load]. Bottom: DC Inductive – Dwell time sweep vs COV_{PP} @ 600 Kilowatts [100% Engine Load].

Figure 16 refers to the co-efficient of variances of IMEP – COV_{IMEP} (a) and peak pressure – COV_{PP} (b) of 300 combustion cycles w.r.t available spark voltage (ASV) sweep at 100% engine load. It was found that once the combustion was stable enough, an increase in ASV did not help in further improving combustion stability. It was also noticed that with smaller sparkplug gaps, it was possible to achieve a robust ignition with a low ASV of 25 kilovolts. However, at higher electrodes gap, high enough voltage was needed to create a break-through – hence an increase in ASV was noticed.

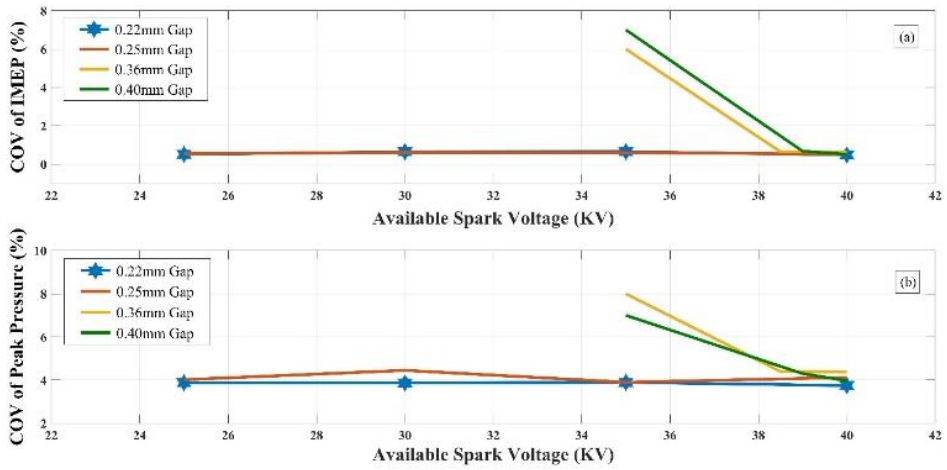

Figure 16: a) AC Capacitive – ASV sweep vs COV_{IMEP}. b) AC Capacitive – ASV sweep vs COV_{PP}.

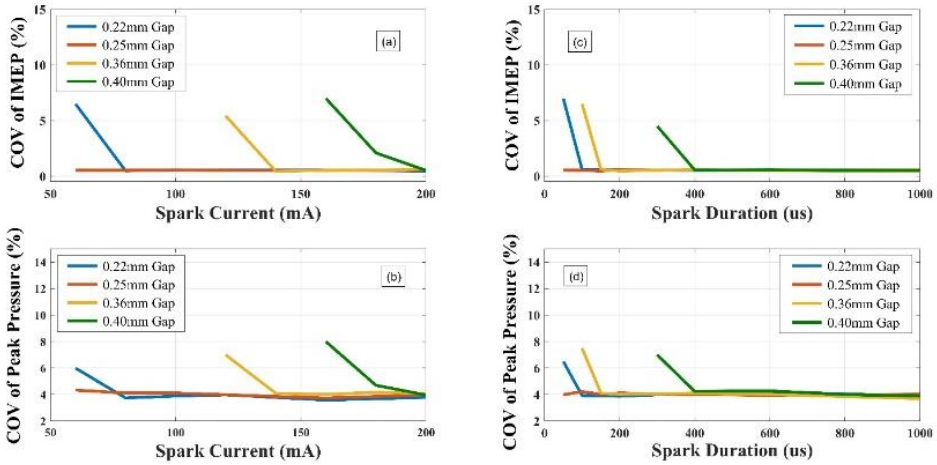

Figure 17:a) & b) AC Capacitive – Spark current sweep vs COV_{IMEP} and COV_{PP}. c) & d) AC Capacitive – Spark duration sweep vs COV_{IMEP} and COV_{PP}.

A further review was made on the combustion stability while sweeping the other two parameters available to design the spark at the same EOP. Figure 3 (a) and (b) shows the COVIMEP and COVPP w.r.t 'spark current' sweep while Figure 5 (c) and (d) w.r.t 'spark duration' sweep. In similar to the observations made during ASV sweep, an increase in both spark current and duration did not support in further improving both COVIMEP and COVPP once the combustion became stable enough.

Similar observations were also made while comparing both the combustion stability and early flame development time at 660 kilowatts brake power (110% engine load). Therefore, it is comprehended that once the flame kernel is developed and starts to propagate, it is independent of the additional spark energy, discharged at the gap.

Conclusions

Studies on ignitability tests have been performed on a medium bore gas engine. The experiments were conducted using two different ignition systems (AC vs DC) while varying the sparkplug electrode gaps. Combining the experimental observations with theoretical reasoning, the following conclusions can be drawn:

- Spark energy is not a relevant measure of the ignitability capability of an ignition system. It is the combination of different spark design parameters that together defines ignitability potential of an ignition system.
- Once a robust and self-sustained combustion is initiated, there is nothing more to gain by further increasing spark energy at the gap. The initial flame kernel becomes independent of the spark energy as soon as it is stable enough to propagate to the rest of the combustion chamber.
- The importance of different degrees of freedom to design a spark has been explored. It is found that a very short spark is enough to robustly ignite the fuel-air mixtures at most EOPs. By effectively controlling multiple spark design parameters, the engine can still achieve a robust combustion with minimal duration of spark. Therefore, a major reduction in excessive spark energy discharge is possible by using a smart ignition system.
- An increase in the electrodes gap increases the demand voltage (at break-through), current and duration in order to achieve a robust ignition. Hence, the optimality of the spark profiles varies with the change in sparkplug gaps.

An Investigation on Spark-Plug Electrodes Wear

Researcher: Anupam Saha
Supervisor: Per Tunestål

Objective

A measurement campaign on sparkplug wear has been performed on a dedicated test-rig at Wärtsilä. The objective of this research is to investigate the influence of different spark energy profiles on sparkplug electrodes erosion over time.

Introduction

This study is a continuation of previous research on ignitability of SI medium bore gas engines. The trade-off between ignitability and sparkplug life is known, since ignitability is often improved by maximizing the energy transfer to the gas at the spark plug gap and minimizing the heat losses to the electrodes during flame-kernel generation and flame growth [16, 17]. However, this enhances the spark plug electrode erosion, shortening its service life.

Therefore, a dedicated investigation has been performed on a test-rig by comparing a conventional DC ignition system with a novel AC ignition system, where the spark characteristics can be controlled by additional degrees of freedom. More specifically, this experiment campaign has been dedicated to study how the AC ignition system and its additional degrees of freedom affect sparkplug wear.

Methodology

A dedicated test-rig was used for continuous test run to study sparkplug wear over time. It was a constant volume vessel and the pressure of medium (air) inside the vessel was regulated by means of a pneumatic system to closely mimic the actual engine conditions at different sparkplug gaps. All the sparkplugs tested in the rig were of dual iridium standard J-gap designs. Initially, the DC Inductive ignition system was mounted on the test-rig, together with a new 0.25 mm sparkplug. The pressure in the chamber was adjusted to achieve the target break-through voltage, as recorded from the ignitability tests. Once the target break-through voltage was achieved, the spark profile was set together with a spark frequency of 6.25 Hertz (~ 750 RPM). The test was operated for 200 hours while the break-through voltage was measured and recorded at multiple time intervals. Once the experiment was over, a new sparkplug of 0.36 mm gap and the experiments were then repeated. Similar procedures were also followed while testing the spark energy profiles using the AC Capacitive ignition system.

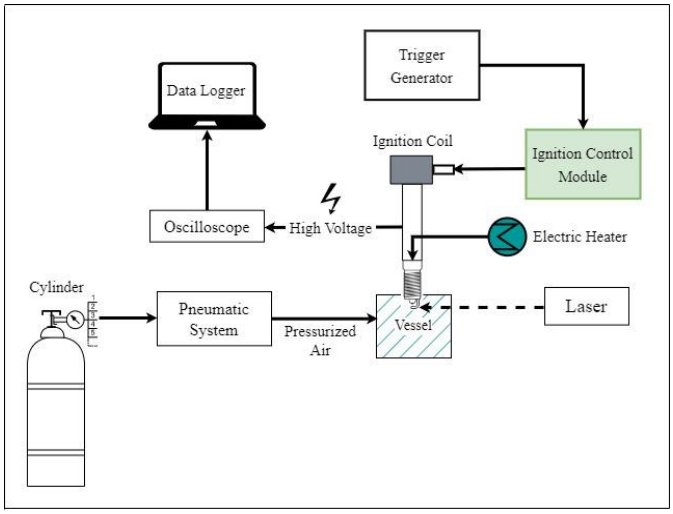

Figure 18: A schematic diagram of the test rig.

Results

Figure 19 shows the comparison of break-through voltage (a), and its rise rate - $\frac{dV}{dT}$ (b) versus the run time of the experiments at 0.25 mm gap. It was found that the rise in break-through voltage (over time) using the DC Inductive was comparatively higher than the AC capacitive ignition system. In addition, it was not possible to operate the DC Inductive system with the same spark energy profile after 168 hours of continuous run. This is probably due to high erosion of sparkplug electrodes, leading to spark misfire after 168 hours of testing.

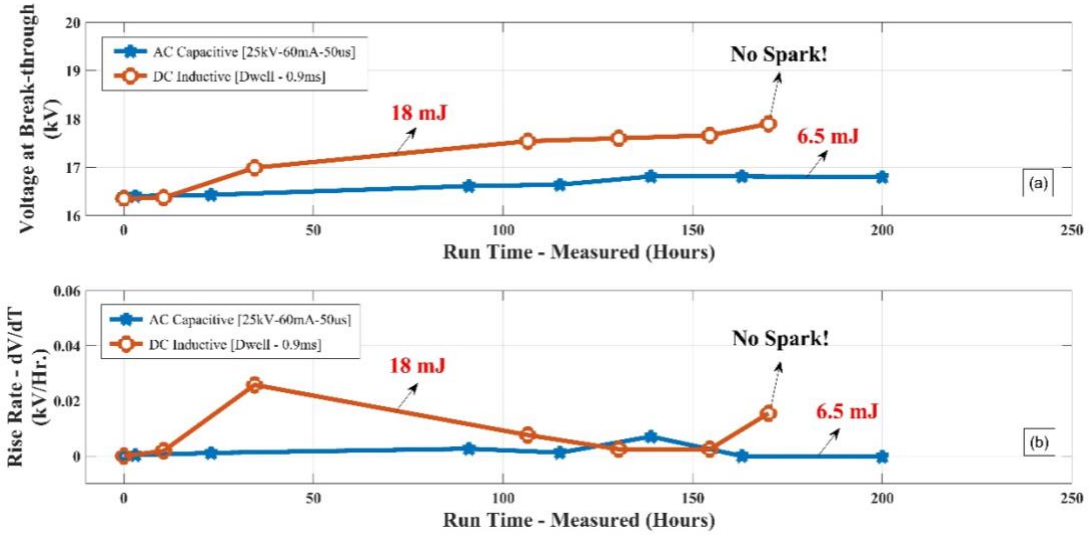

Figure 19: a) Comparison of Break-through Voltage vs Run time @ 0.25 mm gap. b Comparison of Rise-rate of Break-through Voltage vs Run time @ 0.25mm gap).

Similar observations were also found while studying the results from other sparkplug electrode gaps, as seen in Figure 20 and Figure 21.

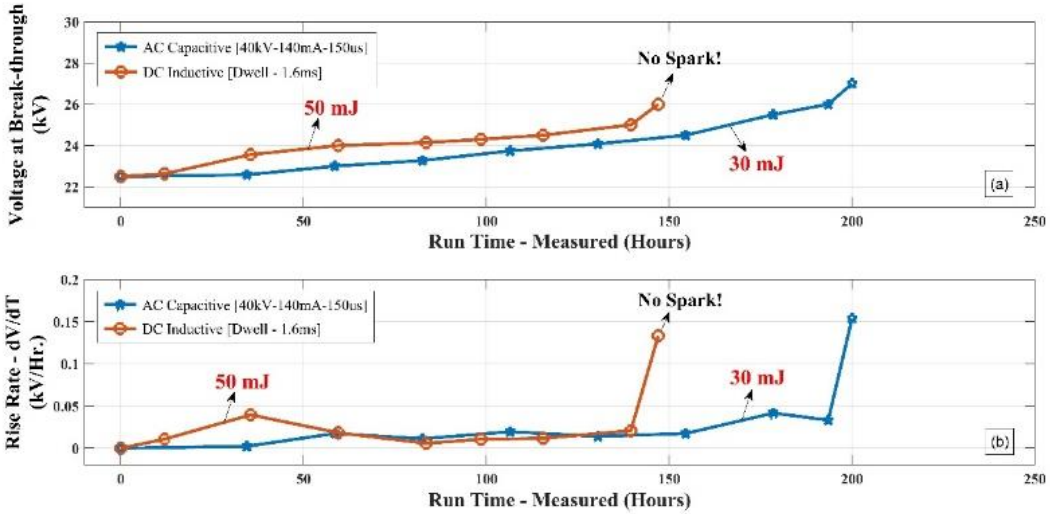

Figure 20: a) Comparison of Break-through Voltage @ 0.36 mm gap . b) Comparison of Rise-rate @ 0.36 mm gap.

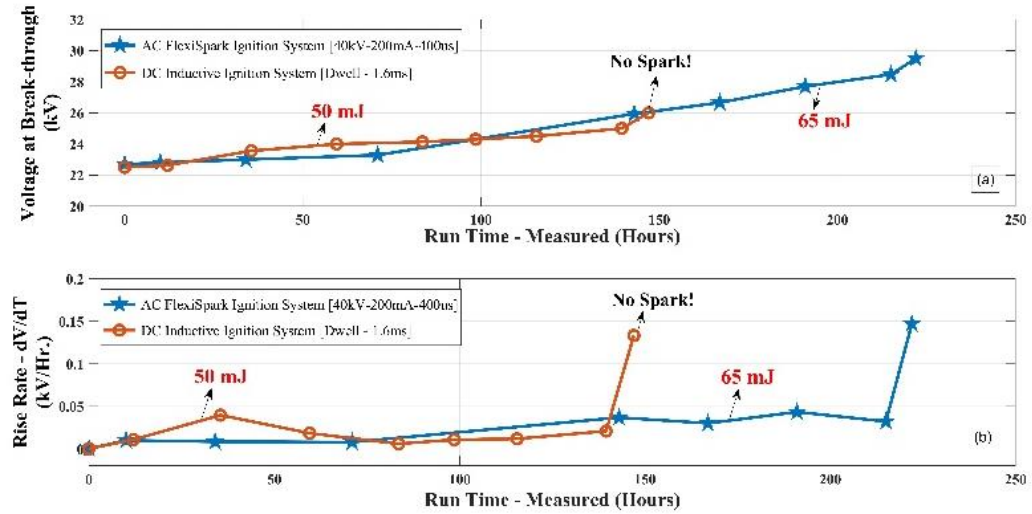

Figure 21: a) Comparison of Break-through Voltage @ 0.40 mm gap. b) Comparison of Rise-rate @ 0.40 mm gap.

The results from sparkplug wear tests have well established the importance of designing ignition by effectively controlling multiple spark discharge parameters. However, it is still unknown whether an AC spark is better than a DC spark in reducing sparkplug erosion. Therefore, an additional experiment was conducted with the AC Capacitive ignition system at 0.25 mm gap using a high spark energy profile.

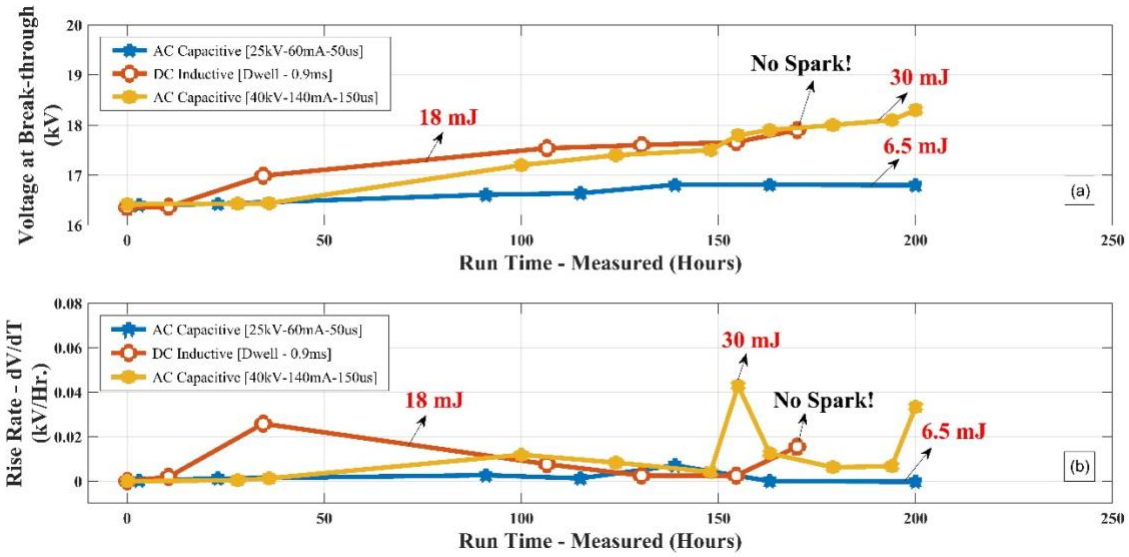

Figure 22: a) Additional Findings - Comparison of Voltage at break-through @ 0.25 mm Gap. b) Additional Findings - Comparison of Rise-rate of Voltage at break-through @ 0.25 mm Gap.

It can be seen from Figure 5, the rise in break-through voltage (over time) using a high energy spark (30 mJ) from the AC capacitive was slow and consistent, compared to the lowest spark energy (18 mJ) profile of the DC Inductive system. Therefore, it is concluded that an AC ignition system has the potential to increase the lifetime of a sparkplug by slowing down the erosion of electrodes over time, as seen from the figure above. Furthermore, the results also indicate that spark energy is not solely responsible for sparkplug erosion. It is also the type of spark discharge (DC/AC) that governs the electrodes wear over time.

Conclusions

Studies on sparkplug wear have been performed on a dedicated test-rig. The experiments were conducted using two different ignition systems (AC vs DC) while varying the sparkplug electrode gaps. Combining the experimental observations with theoretical reasoning, the following conclusions can be drawn:

- The measurement of voltage at break-through with respect to time at a given operating condition is a good indicator of the sparkplug electrodes wear. The results indicate that the DC Inductive system provides faster rise in voltage (high electrodes wear) due to its limited degrees of freedom to control and design the spark. On the contrary, the AC Capacitive ignition system is capable of slowing down the sparkplug wear over time, due to its spark design flexibility.
- The potential of an AC spark discharge over DC is well established through the results obtained from experiments. Due to the inherent property of an AC spark, the direction of the current flow continuously switches between the electrodes. This phenomenon significantly reduces electrodes wear over time, hence increasing the service life of a sparkplug.
- An addition of spark energy (more than sufficient) at the gap contributes to high erosion of sparkplug electrodes, hence reducing the lifetime of a sparkplug. However, spark energy cannot solely be blamed for sparkplug erosion. It is also the type of spark discharge (DC/AC) that governs the electrodes wear over time.

***Note**:* Although the test-rig used in sparkplug wear tests closely simulates the engine conditions, the results do not provide information on sparkplug erosion due to oxidation or hot corrosion – an important phenomenon during an engine operation.

Novel algorithm for peak pressure location estimations using ion current measurements.

Objectives

The aim is to develop and verify ion current based peak pressure location (PPL) algorithm and compare it to existing method.

Introduction

Last year a lot of progress was made on the engine and data acquisition system. The plan for 2022, were too progress the research. Unfortunately, due to long shipment delays of a sensor this has not been the case. During this time, the focused have been to develop the code and method for the coming research and we are expecting to be able to proceed by the end of this year.

During the development of the data acquisition code, we used an algorithm to estimate the time delayed between two signals. By repurposing this algorithm, we were able to develop a novel algorithm to estimate the peak pressure location based on the ion current.

Spark timing plays a vital role in the performance of a spark-ignited engine.
Traditionally the timing is controlled in open-loop, based on lookup tables set during calibration. However, with fuels such as natural gas/biogas certain parameters, e.g. heat release rate and proneness to knock, may vary. This leads to efficiency losses when the fuel deviates from nominal due to incorrect combustion phasing. By developing robust algorithms to estimate the combustion phase and to detect knock we want to implement closed-loop control of the spark timing, thereby being able to account for varying fuel properties.

Novel PPL Algorithm

The newly developed peak pressure location estimation algorithm works in the Fourier domain. The Fourier domain has certain benefits. It is robust to impulse noise in the time domain, the Fourier Transformation is also computationally efficient. However, the key benefit of the novel algorithm is the fact that it can give a PPL estimation each cycle, which was not feasible with the previous algorithm. This makes it more favorable when combining with for example knock detection and control, where it is desired to perform control on a cycle by cycle basis.

Methods

The ion current is measured in each cylinder, using the spark plug as a sensor. The peak pressure location is then estimated and validated using the in-cylinder pressure trace, and performance is compared with the old PPL estimation algorithm.

Results

The novel PPL estimation works, and shows an improvement over the previous method.

Comparison between the old and novel method in different operating points can be found in Table 2 below. The results from cycles in which the old method could not give an estimation of PPL are shown in Table 3.
Note that the standard deviation of the error is smaller for the novel algorithm in every operating point tested.

Table 2: Comparison between the new and old method at different operating points. The compared metrics are average error of the PPL estimations and the error standard deviation.

Operating Point		Result Novel algorithm		Result Old Algorithm	
RPM	Torque	Avg Err	Err Std	Avg Err	Err Std
1000	1000	.240	.770	-.490	.938
1000	1250	-.042	.788	-.454	.967
1000	1500	.070	.817	-.342	1.066
1100	1000	.362	.835	-.643	.989
1100	1250	-.083	.849	-.489	1.039
1100	1500	.234	.842	-.422	1.100
1200	1000	.211	.842	-.579	1.021
1200	1250	-.107	.869	-.448	1.039
1200	1500	.073	.836	-.496	1.082

Table 3: The results from the new method for cycles where the old method could not give a PPL estimation.

Operating Point		Result Novel algorithm	
RPM	Torque	Avg Err	Err Std
1000	1000	.143	.971
1000	1250	-.156	1.135
1000	1500	-.010	1.137
1100	1000	.294	1.108
1100	1250	.006	1.083
1100	1500	-.146	1.179
1200	1000	.114	1.084
1200	1250	-0.004	1.126
1200	1500	-.162	1.177

Conclusions

By the end of this year we are expected to be fully operational and conducting research. The novel PPL algorithm shows promising results, but further test of robustness needs to be made to ensure that it works for a larger span of operating points.